**Stress Changes the Bacterial Biomolecular Condensate Material State and Shifts Function from mRNA Decay to Storage**

Luis A. Ortiz-Rodríguez[1], Hadi Yassine[2], Vidhyadhar Nandana[2], Christopher A. Azaldegui[3], Jiayu Cheng[1], Jared M. Schrader[2*], Julie S. Biteen[1,3*]

[1]Department of Chemistry, University of Michigan, Ann Arbor, MI 48109 USA.

[2]Departments of Chemistry and Biological Sciences, Wayne State University, Detroit, MI 48202 USA.

[3]Doctoral Program in Chemical Biology, University of Michigan, Ann Arbor, MI 48109, USA.

[*]To whom correspondence should be addressed: jsbiteen@umich.edu, schrader@wayne.edu

**Abstract**

Bacterial ribonucleoprotein bodies (BR-bodies) are dynamic biomolecular condensates that play a pivotal role in RNA metabolism. We investigated how BR-bodies significantly influence mRNA fate by transitioning between liquid- and solid-like states in response to stress. With a combination of single-molecule and bulk fluorescence microscopy, biochemical assays, and quantitative analyses, we determine that BR-bodies promote efficient mRNA decay in a liquid-like condensate during exponential growth. On the other hand, BR-bodies are repurposed from sites of mRNA decay to reservoirs for mRNA storage under stress, a functional change that is enabled by their transition to a more rigid state, marked by reduced internal dynamics, increased molecular density, and prolonged residence time of ribonuclease E. Furthermore, we manipulated ATP levels and translation rates and conclude that the accumulation of ribosome-depleted mRNA is a key factor driving these material state transitions, and that condensate maturation further contributes to this process. Upon nutrient replenishment, stationary-phase BR-bodies disassemble, releasing stored mRNAs for rapid translation, demonstrating that BR-body function is governed by a reversible mechanism for resource management. These findings reveal adaptive strategies by which bacteria regulate RNA metabolism through condensate-mediated control of mRNA decay and storage.

**Introduction**

Biomolecular condensates are dynamic macromolecular assemblies that often form via phase separation,[1,2] a reversible process that enables the cell to respond rapidly to environmental changes.[3] These assemblies are selectively permeable and can exchange client molecules.[1,4] Depending on their physical state, which can range from liquid droplets to hydrogels and insoluble aggregates, condensates facilitate various biological functions.[1,5] Liquid-like condensates promote biochemical reactions by allowing internal diffusion and exchange with the dilute phase, while gel- and solid-like condensates have reduced diffusion and exchange, which slow down biochemical reactions and may potentially sequester biomolecules for

storage.[1,2] Notably, transitions from the liquid to solid state in biomolecular condensates have been linked to neurodegenerative protein aggregation disorders:[6,7] reducing the fluidity of these condensates can negatively affect their function.[8,9] However, in other cases, such as germ granules, solid-like states play important roles in mRNA storage and translational control in the developing embryo.[10]

Recently, biomolecular condensates have emerged as a broadly utilized mechanism for organizing diverse biochemical pathways within the bacterial cytoplasm,[11–19] and this organizational paradigm is particularly important in bacteria because these organisms generally lack membrane-bound organelles.[20,21] Bacterial ribonucleoprotein bodies (BR-bodies), the organelles that contain the RNA degradation machinery, were the first bacterial condensates demonstrated to assemble via liquid-liquid phase separation (LLPS), driven by interactions between the large intrinsically disordered region (IDR) of ribonuclease E (RNE; Fig. 1a) and RNA.[11]

*Caulobacter crescentus* BR-bodies share functional similarities with eukaryotic processing bodies (P-bodies) and stress granules (SGs) as all three promote mRNA decay. RNE (Fig. 1a), the core scaffold and driver of BR-body function, is the essential and rate-limiting factor in bacterial mRNA decay.[22,23] Similarly, Xrn1 is a core component of eukaryotic P-bodies and SGs, and it controls cytoplasmic mRNA decay.[24–26] In addition, similar types of molecules are enriched in BR-bodies (Fig. 1b,c), P-bodies, and SGs, including DEAD-box RNA helicases, Lsm proteins, miRNAs, small-RNAs, and translationally repressed mRNAs.[27] P-bodies and SGs have been predominantly studied under conditions of cell stress, and some studies indicate that P-bodies promote mRNA decay while others show an mRNA storage function, whereas SGs have only been found to promote storage.[11,25,28] These differences in the decay and storage functions are correlated with differences in the mobility of molecules within P-bodies[25,28–31] and SGs,[32–34] since P-bodies have been found to have higher mobility and more rapid exchange with the dilute phase than SGs. BR-bodies have been predominantly studied in exponentially growing bacteria cells, during which they appear to have liquid-like properties that promote mRNA decay (Fig. 1c).[11,35] In contrast, under cell stress, BR-bodies undergo

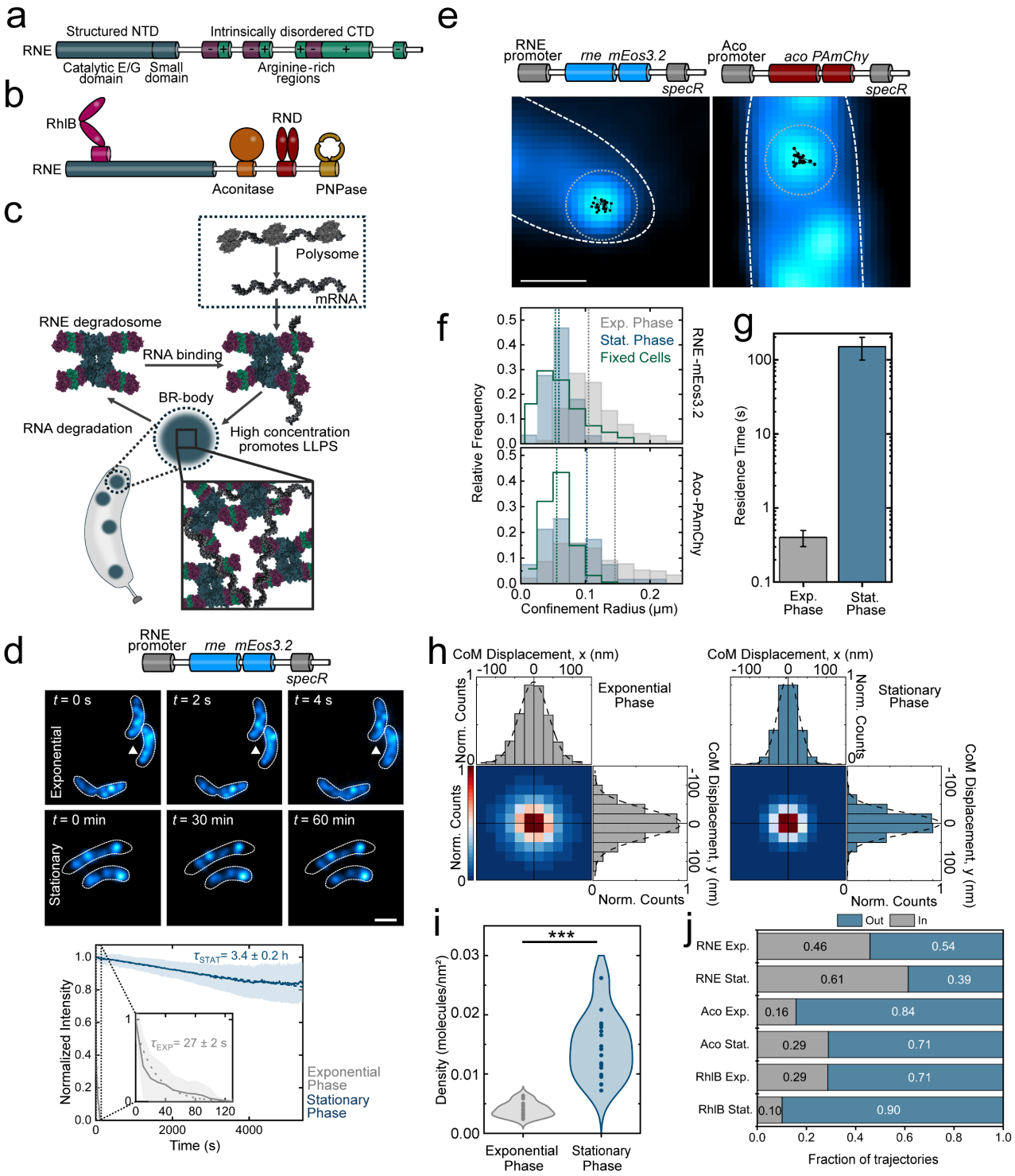


**Fig. 1 | BR-bodies are dynamically arrested and compacted upon entering the stationary phase.**

**Fig. 1 | BR-bodies are dynamically arrested and compacted upon entering the stationary phase**. (a) Domain organization of *C. crescentus* RNase E (RNE). (b) The *C. crescentus* RNA degradosome includes RNE, RhlB, aconitase, RNase D, and PNPase. The RNE NTD has an RhlB binding site. The CTD has interaction sites for aconitase, RNase D, and PNPase. (c) In the working model for BR-body-mediated mRNA decay, untranslated mRNAs and the RNE degradosome can phase separate into a biomolecular condensate, thereby increasing their local concentration and accelerating decay processes within the BR-body. The condensate dissolves as mRNA is degraded, releasing degradosome components and oligonucleotides. (d) Lifespans of condensates based on an RNE-mEos3.2 construct (top). Middle: representative images of *C. crescentus* cells (white outlines) and RNE-mEos3.2 (blue) in each phase as a function of imaging time, *t*; arrowheads indicate representative RNE-mEos3.2 foci. Scale bar: 500 nm. Bottom: decay profiles of photobleaching-corrected intensities with estimates of the average condensate lifespans, $\tau_{EXP}$ and $\tau_{STAT}$, in the exponential and stationary phases, respectively. Analyses include $N = 427$ foci (exponential) and $N = 932$ foci (stationary). (e-j) Dynamics of degradosome components within BR-bodies across growth phases. (e) Single-molecule tracking of degradosome components inside BR-bodies. Top: genetic constructs used to track RNE and aconitase. Bottom: representative single-molecule trajectories of RNE-mEos3.2 (left) and aconitase-PAmChy (right) within BR-bodies (dotted circles) in *C. cresentus* cells (dashed lines). The black dots indicate the super-localized positions of the molecule in consecutive 20-ms imaging frames. Scale bar: 500 nm. (f) Changes in the diffusivity of degradosome components within BR-bodies across growth phases. The distributions of confinement radii for RNE-mEos3.2 and Aco-PAmChy trajectories in live cells are compared to apparent confinement radii of trajectories in fixed cells to distinguish between diffusing and static molecules. Vertical dotted lines: distribution medians. (g) Increase in residence time of RNE-mEos3.2 of BR-bodies between exponential and stationary phase. (h) Decrease in BR-body size between the exponential and stationary phases. The BR-body size is estimated from single-molecule displacements relative to the center of mass (CoM) of each RNE-mEos3.2 trajectory within a BR-body during each phase. (i) Increase in the density of RNE-mEos3.2 single-molecule localizations within BR-bodies during the transition from exponential to stationary phase. Each point represents the density in one condensate. (j) The fraction of degradosome components RhlB-PAmChy, Aco-PAmChy, and RNE-mEos3.2 inside (grey) and outside (blue) the BR-bodies is a function of the growth phase, indicating the presence of incomplete degradosomes in BR-bodies during the stationary phase.

increased condensation that correlates with enhanced survival under these conditions, yet their internal dynamics and rates of mRNA degradation have not previously been explored under stress.[11] Evidence from multiple bacterial species has shown that mRNA decay rates are reduced under conditions of nutrient limitation, such as when cells enter the stationary phase, yet the role of BR-bodies in this slowdown of mRNA decay has not yet been explored.[36–41]

In this study, we investigate changes in the dynamics within BR-bodies between exponential growth and stationary phase and how these differences impact the mRNA decay pathway. Our live-cell single-molecule microscopy results demonstrate that BR-bodies transition from a dynamic, liquid-like state during exponential growth to a less dynamic, more rigid state during stress. We demonstrate that this transition is associated with a functional shift from enhancing mRNA decay in the exponential phase to promoting mRNA storage in the rigid state. In line with these results, we measure that the *in vitro* maturation of RNE condensates and subsequent arrest of dynamics lead to a strong reduction in RNE activity. Given the similarities between BR-bodies and eukaryotic biomolecular condensates like SGs and P-bodies, our findings further suggest that differences in cell growth conditions may also alter the material properties of P-bodies and SGs to shift the inherent preferences for mRNA decay vs. storage across diverse organisms.

**The exponential to stationary phase transition induces a rigid BR-body material state**

To investigate the dynamics of molecules within BR-bodies and their response to stress, we labeled the endogenous copy of RNE with the green-to-red photoconvertible fluorescent protein mEos3.2 (RNE-mEos3.2; Fig. 1d).[42] This labeling strategy allows us to study the properties of BR-bodies as a whole using bulk fluorescence in the initial mEos3.2 green state, and to measure their internal dynamics at the single-molecule level in the mEos3.2 red state after photoconversion using 405-nm excitation. We compared BR-body dynamics during the exponential and stationary growth phases to understand the effect of non-invasively induced cellular starvation, ensuring physiologically relevant observations of the stress response.

We further sought to resolve two previous confounding observations: (1) there is an increased number of BR-bodies and a higher copy number of RNE in each condensate in cells at the stationary phase,[11] a nutrient-deprived state during which bacterial growth and division cease, and yet (2) mRNA decay is slower in the stationary phase.

To investigate how the stationary phase alters BR-bodies, we performed time-lapse imaging of cells in the exponential and stationary phases. In the exponential phase, BR-bodies rapidly assemble and disassemble, consistent with their known role in mRNA decay (Fig. 1d). However, in the stationary phase, BR-bodies are dramatically stabilized (450-fold; Fig. 1d). As RNA is required for BR-body phase separation,[11] the decreased dissolution rate of BR-bodies during stationary phase suggests reduced RNA decay activity, as mRNA degradation is necessary for BR-body disassembly (Fig. 1c).[11] Single-molecule tracking of RNE-mEos3.2 and the degradosome protein aconitase-PAmChy, previously identified as a direct binding partner to RNE[11,43,44] revealed significantly reduced diffusivity of RNE and its degradosome client proteins within BR-bodies during the stationary phase (Fig. 1e,f), consistent with a more rigid internal microenvironment. Furthermore, the residence time of RNE within BR-bodies is 370-fold longer in the stationary phase compared to the exponential phase (Fig. 1g). By analyzing the single-molecule displacements per 20 ms relative to the center of mass (CoM) of each RNE-mEos3.2 trajectory within the BR-bodies, we estimated the cluster diameters (Fig. 1h). Additionally, using density-based cluster analysis,[45] we determined the molecular density (Fig. 1i) in the RNE clusters during both growth phases. In the exponential phase, BR-bodies are less dense and larger ($d_{FWHM}$ = 101 ± 3 nm) than in the stationary phase ($d_{FWHM}$ = 84 ± 2 nm). Importantly, the decreased diffusivity and increased residence time of RNE within the BR-bodies, along with their compaction, are also observed under ethanol stress, indicating that dynamic arrest behavior likely occurs under other inducing stresses (Extended Data Figs. 1,2). This compaction explains the decreased internal dynamics, where the rigid state constrains RNE within the BR-body.

BR-bodies are enriched in the RNA degradosome complex, which in *C. crescentus* contains aconitase, RhlB, and PNPase (Fig. 1b).[11,44] We analyzed the localization of the degradosome proteins aconitase and RhlB and observed significant changes in their recruitment to BR-bodies following the transition to a more rigid material state during the stationary phase (Fig. 1j). Specifically, the recruitment of RNE and aconitase increases, while the recruitment of the DEAD-box RNA helicase RhlB significantly decreases. These results suggest that rigidification leads to an altered RNA degradosome in BR-bodies during the stationary phase. DEAD-box RNA helicases are central regulators of biomolecular condensates;[46] their ATPase cycle maintains the condensates in a dynamic, non-equilibrium state, facilitating the enrichment of client molecules and buffering the dispersed ribonucleoprotein pool. The decreased recruitment of RhlB thus likely impairs the internal remodeling of BR-bodies, potentially contributing to their rigidification during stress.

**Increased levels of poorly translated mRNA and maturation trigger the transition to the rigid material state**

During the stationary phase, bacterial cells encounter nutrient scarcity, which slows down cellular processes including metabolic activity, leading to lower ATP levels (Fig. 2a).[47] Reduced ATP levels subsequently impact various processes, including protein synthesis and translation, promote phase separation of proteins with intrinsically disordered regions (IDRs),[18] contribute to protein aggregation,[12,13] and cause physical changes in cytoplasm,[48,49] creating a glassy state that slows the diffusion of mesoscale objects such as BR-bodies. Additionally, since DEAD-box helicases like RhlB require ATP hydrolysis to remodel, dissolve, prevent strong interactions, and maintain the fluidity of the condensates,[46] the low ATP levels at the stationary phase may impair these activities.

To separate the effects of low ATP levels and reduced translation on BR-body rigidification, we artificially decreased ATP and translation levels in exponential phase cultures of *C. crescentus*.

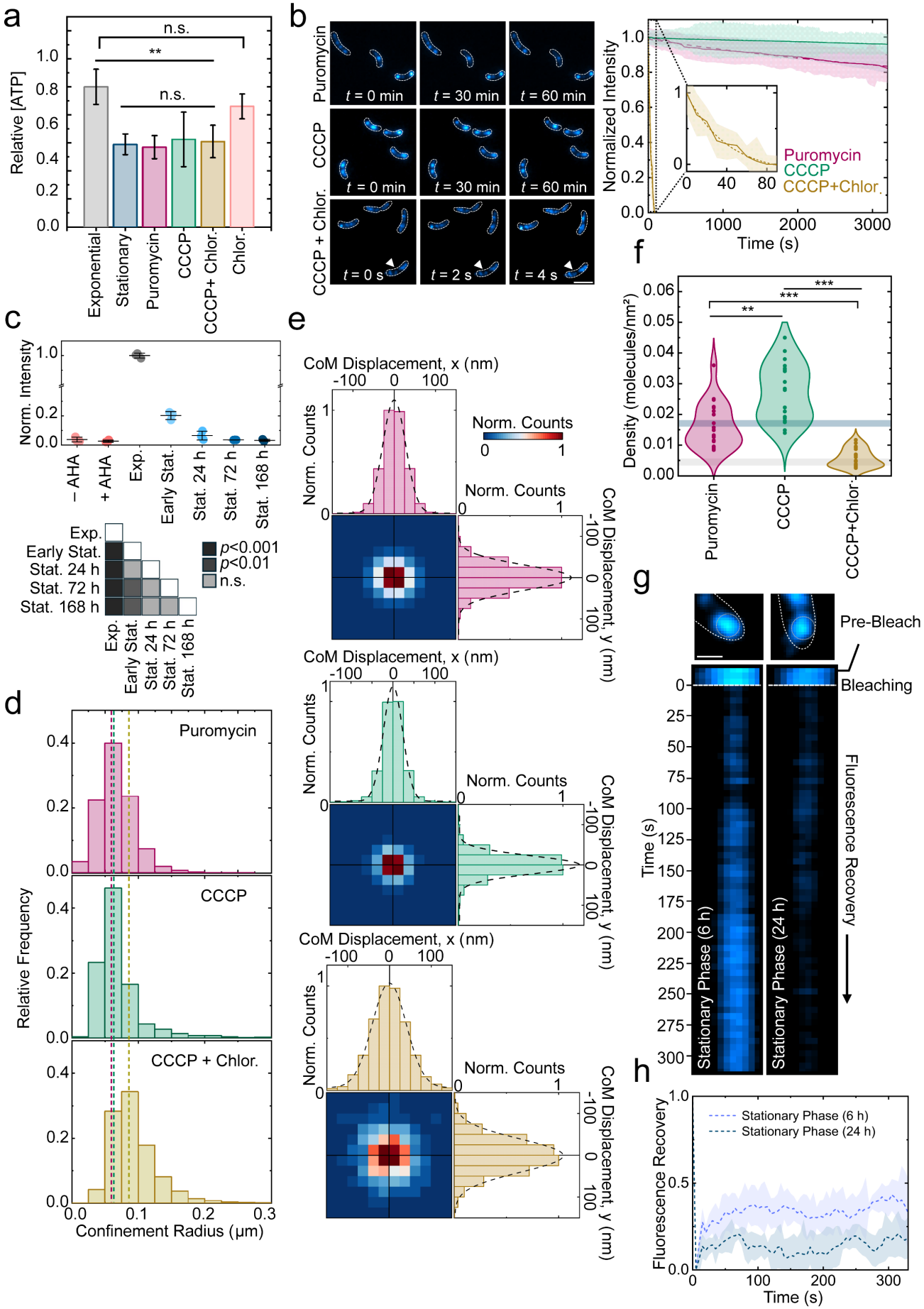


**Fig. 2 | Rigidification of BR-bodies is promoted by increased levels of poorly translated mRNAs.**

**Fig. 2 | Rigidification of BR-bodies is promoted by increased levels of poorly translated mRNAs**. (a) Quantification of intracellular ATP concentrations in *C. crescentus* using a luciferase-based assay following no treatment or treatment as described. ATP levels are normalized to exponential growth levels. Error bars: standard deviation from three biological replicates. ** denotes $p < 0.005$ and n.s. denotes $p > 0.05$. (b) Lifespans of BR-bodies in cells under the acute treatment conditions described in (a). Left: Representative images of RNE-mEos3.2 (blue) in *C. crescentus* cells (white outlines) as a function of treatment and imaging time, *t*. Arrowheads indicate representative RNE-mEos3.2 foci. Scale bar: 2 μm. Right: Decay profiles of photobleaching-corrected intensities used to estimate the average condensate lifespan. Analyses include $N$ = 308, 347, and 241 foci for puromycin, CCCP, and CCCP + chloramphenicol, respectively. (c) Top: relative translational levels in the exponential and stationary phases using Biorthogonal Non-Canonical Amino Acid Tagging (BONCAT), and controls with azidohomoalanine (AHA) and chloramphenicol and without AHA. Error bars: standard deviation of three replicates. Bottom: statistical analysis. (d) Impact of acute treatments on the diffusivity of the BR-body RNE scaffold. The distribution of confinement radii for RNE-mEos3.2 trajectories is measured following each treatment. Vertical dashed lines: distribution medians. (e) Effect of acute treatments on the BR-body size, which is estimated from displacements relative to the center of mass (CoM) of each RNE-mEos3.2 trajectory following each treatment. (f) Changes in the density of RNE-mEos3.2 single-molecule localizations within BR-bodies following each treatment. (g) Dynamics inside BR-bodies in cells during prolonged stationary phase. Representative fluorescence recovery after photobleaching (FRAP) experiment kymographs during early (6 h) and late (24 h) stationary phase cells showing the bleaching and recovery of the RNE-mEos3.2 foci (blue) as a function of time, *t*. Scale bar: 500 nm. (h) FRAP of RNE-mEos3.2 in cells at the early and late stationary phase. $N$ = 20 foci.

To lower ATP levels, we treated the cultures with the protonophore carbonyl cyanide *m*-chlorophenyl hydrazone (CCCP) to disrupt the proton motive force,[50] rapidly inhibiting ATP synthase. A 20-min treatment with 100 μM CCCP was found to reduce cellular ATP concentrations to levels comparable to those observed during the stationary phase (Fig. 2a). To reduce translation levels, we used puromycin (150 μg/mL for 30 min), which prematurely cleaves peptide chains[51] and releases ribosome subunits and mRNA, thereby increasing the availability of ribosome-depleted transcripts in the cytoplasm. Since puromycin treatment also results in ATP levels similar to those observed in the stationary phase (Fig. 2a), we treated cells with CCCP and the translation elongation inhibitor chloramphenicol as a control. Chloramphenicol prevents translation by blocking peptide bond formation and accumulating ribosomes on mRNA.[52] Interestingly, treating exponential phase cultures with CCCP and puromycin leads to long-lived BR-bodies (Fig. 2b), similar to those observed during the stationary phase (Fig. 1d). However, when cells are treated with the combination of CCCP and chloramphenicol, BR-bodies remain short-lived, similar to those observed during the exponential phase in the absence of stress (Fig. 2b). This finding suggests that the increased lifespan of BR-bodies upon treatment with CCCP might be an indirect effect of dropping ATP levels inhibiting translation rather than directly related to the ATP availability. Translation is typically the most energy-intensive process during exponential growth,[53,54] and ATP and GTP are essential for several steps in translation, including the esterification of amino acids to tRNAs, delivery of the aa-tRNAs to the ribosome, the assembly of ribosomal subunits, and the translocation of ribosomes along the mRNA. When NTP levels are decreased, these processes slow, resulting in reduced translation rates. Additionally, biorthogonal non-canonical amino acid tagging (BONCAT) revealed a significant decrease in translation levels during the late stationary phase, with reductions of 30-fold, as well as in cells treated with puromycin, CCCP, and the combination of CCCP and chloramphenicol, all relative to the exponential phase (Fig. 2c, Extended Data Fig. 3).

Similar to the extended lifespan of BR-bodies observed upon treatment with CCCP and puromycin, these treatments also replicated the stationary-phase decreases in RNE-mEos3.2 diffusivity inside the BR-bodies (Fig. 2d), BR-body size (Fig. 2e), RNE molecular density (Fig. 2f), and residence time within BR-bodies (Extended Data Fig. 2). Conversely, cells treated with a combination of CCCP and chloramphenicol do not rigidify. This finding suggests that the rigid material state transition in the stationary phase state requires increased amounts of ribosome-free mRNA transcripts in the cytoplasm, whereas ATP scarcity alone is insufficient.

We identified low ribosome occupancy as a key factor contributing to the rigid material state of BR-bodies during the stationary phase. However, under prolonged stress, biomolecular condensates have been observed to mature from having liquid-like to solid-like properties.[1,55–59] Initially, their components interact transiently: molecules freely rearrange and exchange with the surrounding phase, resembling liquid behavior. Over time, mechanisms such as entanglement of disordered polypeptides,[60] vitrification,[61] percolation,[62] and nucleation and elongation of amyloid-like fibers[63] contribute to rigidification and decreased molecular dynamics.[64] We investigated the role of maturation in BR-body rigidification by *in vivo* fluorescence recovery after photobleaching (FRAP) of BR-bodies (RNE-mEos3.2) in cultures of *C. crescentus* cells at 6 hrs and 24 hrs into the stationary phase (Fig. 2g,h). The condensates become less dynamic over time in the stationary phase. The BR-body fluorescence recovers only minimally at both time points, consistent with a rigid material state, but BR-bodies are slightly more dynamic at 6 hrs than at 24 hrs. To further investigate the role of maturation, we reconstituted the system *in vitro* and extracted meaningful information based on RNE, the first bacterial protein found to undergo LLPS at physiological concentrations without crowding agents.[11] FRAP performed on RNE droplets reconstituted *in vitro* and aged for 30 min, 4 hrs, and 8 hrs (Extended Data Fig. 4) revealed that condensates aged for 30 min were significantly more dynamic, with nearly full fluorescence recovery within 2.5 min, whereas condensates aged for 4 hrs

exhibited minimal recovery and 8 hrs were even less dynamic. These results support the role of maturation in changing the material state of BR-bodies.

**The material state transition of BR-bodies during stress shifts their function from promoting mRNA decay to facilitating mRNA storage**

Our *in vivo* and *in vitro* results establish that, during stress conditions, the internal dynamics and structure of BR-bodies become more rigid. Previous two-color images of mRNA and RNE using MS2 RNA labeling[65] and fluorescence *in situ* hybridization (FISH) have shown that transcripts such as *rsaA* exhibit low colocalization (~28%) with RNE in BR-bodies during active RNA degradation.[35] However, colocalization increases significantly (~80%) when RNE endonuclease cleavage is blocked using an RNE active site mutation (ASM) involving the two residues coordinating the catalytic $Mg^{2+}$ ion in the active site.[35] These results suggest that the transition to a more rigid material state, along with its associated effects, may enable BR-bodies to store mRNA storage during stress conditions.

To investigate the role of BR-bodies in mRNA storage, we performed two-color imaging of RNE and mRNA using a live-cell MS2 system and FISH, and we measured mRNA degradation rates using quantitative polymerase chain reaction (qPCR). Notably, this study employs an MS2 system optimized to accurately track short-lived mRNAs.[66] We selected four key mRNA transcripts needed for *C. crescentus* exponential growth: *rsaA*, *rne*, *spmX*, and *ctrA*. The RsaA S-layer protein is the most abundant protein in *C. crescentus*[67]. RsaA was chosen to replicate the phenotype observed when RNE cleavage is blocked using the ASM, providing insight into the role of the catalytic activity of RNE in the condensate and its effect on transcript recruitment into BR-bodies.[35] RNE is crucial in RNA processing, degradation,[22,23] BR-body formation, and cell fitness.[11] The integral membrane protein SpmX enables cell division by localizing the histidine kinase DivJ to the stalked pole.[68,69] Finally, CtrA is a master regulator of the cell cycle; it controls chromosome replication and transcription, and it

modulates the expression of about 25% of cell cycle-regulated genes in *C. crescentus*.[70–74] These strategically selected transcripts enabled us to thoroughly assess the role of BR-bodies in mRNA storage under stress and to determine the relevance of the stored transcripts.

Images of MS2-labeled *ctrA*, *spmX*, and *rsaA* transcripts (Fig. 3a,b, and Extended Data Fig. 5) highlight their higher recruitment to BR-bodies during the stationary phase compared to the exponential phase; these data sets were quantified using Pearson correlation coefficients (PCC). All transcripts colocalize more with BR-bodies during the stationary phase, similar to the behavior of *rsaA* when RNE cleavage is blocked, suggesting significantly lower degradation activity by RNE during this phase. This mRNA RNE colocalization is further confirmed by FISH (Extended Data Fig. 6). We also assessed the stability of these transcripts tagged with MS2-RNA hairpins by analyzing the photobleaching-corrected intensities of MS2-mChy foci colocalized with RNE foci during both growth phases (Fig. 3c and Extended Data Fig. 5). To ensure that our observations accurately reflect transcript stabilization and not artifacts of the labeling system, we employed two versions of the MS2 system which are both utilized with a MS2-mChy dimerization deficient variant:[75] a 48×-array with weaker MS2 coat protein RNA hairpin affinity[66] and a 96×-array.[35] Previous studies have demonstrated that binding of the coat protein to MS2 binding sites artifactually stabilizes mRNA.[76–78] Therefore, we confirmed that any observed accumulation of the mChy signal within BR-bodies was due to real transcript stabilization and not an effect of the labeling system. As shown in Fig. 3a,b, mChy foci do not colocalize with BR-bodies during the exponential phase when using the 48×-array system or by mRNA FISH using probes to the coding sequence (Extended Data Fig. 6). However, using the 96×-array version (Extended Data Fig. 5), we observed mChy foci colocalizing with BR-bodies, even during the exponential phase. Despite the potential transcript stabilization caused by the more perturbing 96×-array MS2 system, we still observed significant differences in the decay profiles between exponential and stationary phases. During the exponential phase, MS2-mChy (96×-array) foci

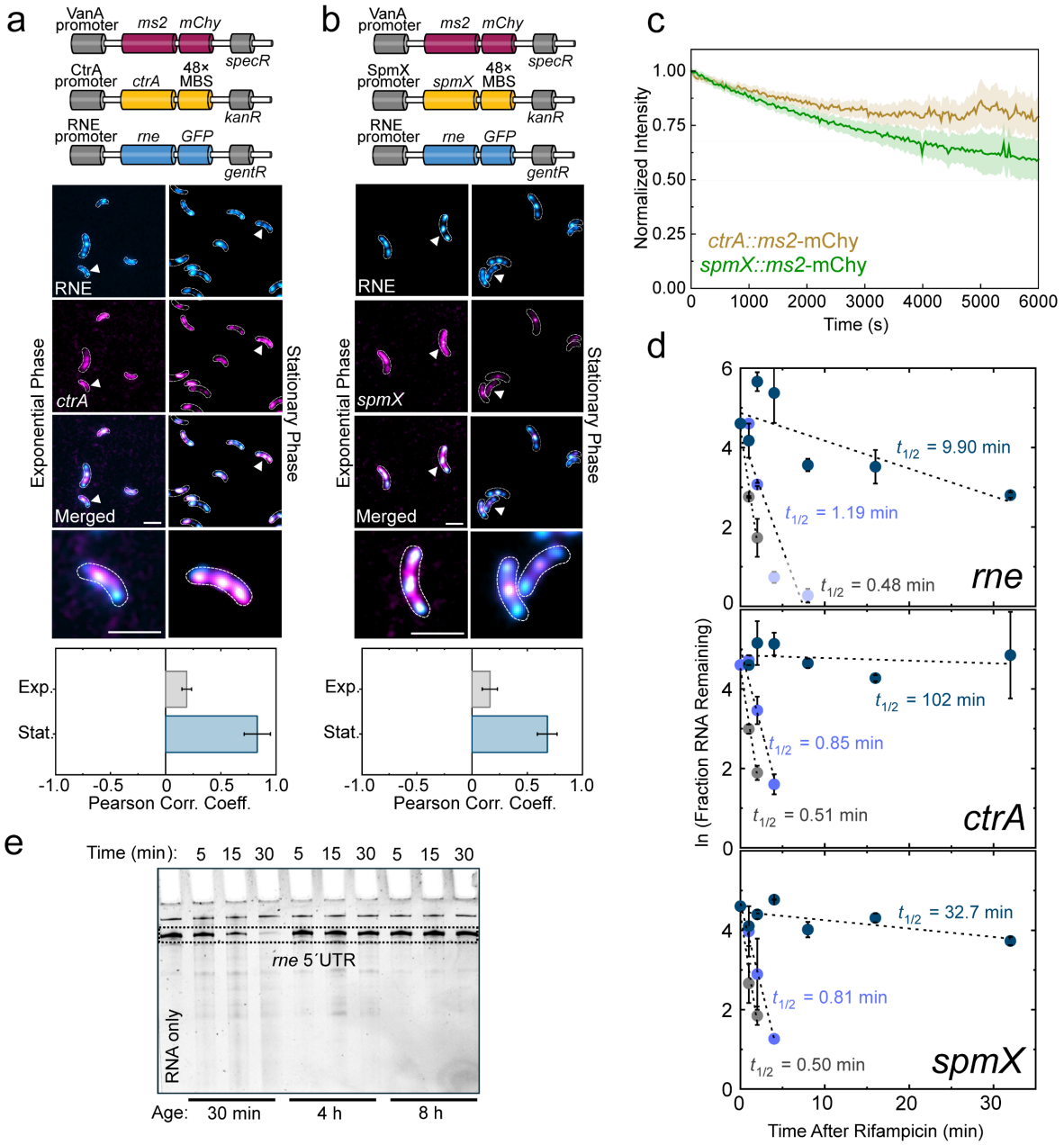


**Fig. 3 | Rigidification of BR-bodies switches their function from mRNA decay to storage of key growth mRNAs.**

**Fig. 3 | Rigidification of BR-bodies switches their function from mRNA decay to storage of key growth mRNAs.** (a,b) Stability of the *ctrA* (a) and *spmX* (b) transcripts in BR-bodies. Top: genetic constructs used to observe the transcript stability within the BR-bodies *in vivo*. Middle: Representative two-color images showing higher recruitment of the *ctrA* and *spmX* transcripts (magenta) to BR-bodies (blue) during the stationary phase (left) relative to the exponential phase (right). The merged channel is shown on two magnification levels for clarity. Bottom: Differences in recruitment quantified by the Pearson correlation coefficients between channels. Error bars: standard deviation from 20 foci analyzed per phase. *** denotes $p < 0.001$. Arrowheads indicate representative foci. Scale bars in (a) and (b): 2 μm. (c) Decay profiles of *ctrA* and *spmX* in the late stationary growth phase. Analyses include $N = 108$ and 174 foci for the *ctrA* and *spmX* transcripts, respectively. (d) qRT-PCR measurements of RNA half-lives for *rne*, *ctrA*, and *spmX* transcripts highlight the changes in transcript stability from the exponential phase to the late stationary phase. Error bars: standard deviation from at least three technical replicates. (e) Condensate aging leads to decreased RNE cutting activity *in vitro*, as evidenced by the *rne* mRNA band in a 7% urea TBE/PAGE gel.

disassemble in under a few min, consistent with rapid internal decay of mRNAs (Extended Data Fig. 5). In contrast, during the stationary phase, MS2-mChy (48×-array) foci stably colocalize with BR-bodies for significantly longer, indicating slowed mRNA decay (Fig. 3c and Extended Data Fig. 5). To investigate the observations of the MS2 tagged RNAs, we measured the RNA decay rates by qRT-PCR. mRNA half-life measurements confirmed this stabilization: *rne*, *spmX*, and *ctrA* exhibit 20-, 65-, and 200-fold increases in stability, respectively, from exponential to late stationary phase (Fig. 3d). Altogether, these measurements suggest that the rigid state of RNE causes a dramatic slowdown in mRNA decay activity.

To investigate whether the reduced RNA cleavage activity of RNE is a direct result of rigidification, we assessed the cutting activity of RNE in 30-min, 4-hr, and 8-hr *in vitro*-reconstituted condensates (Fig. 3e). These aged RNE droplets were formed with RNE and RNA, but without $Mg^{2+}$, an essential cofactor for RNA cleavage by RNE. At each droplet age, RNA cleavage was initiated by adding $Mg^{2+}$, and samples were collected at various time points to assay RNA cleavage.[79] RNE efficiently cleaves the *rne* 5' UTR in droplets aged for only 30 min,[79] with the corresponding band in the PAGE gel disappearing within 30 min of $Mg^{2+}$ addition (Fig. 3e). In contrast, virtually no RNA cleavage was observed in the rigidified droplets at the 4-hr and 8-hr timepoints. This finding suggests that maturation into the rigid state can directly shut off RNE cleavage.

**Fluidized BR-bodies are capable of the functional release of mRNAs**

Stored mRNAs may be useful for growth-arrested cells either by acting as a nutrient source to promote regrowth or by being released to restart the translation program by releasing stored mRNAs to ribosomes upon the addition of new nutrients. To determine if mRNA release and subsequent translation can occur after cells exit the stationary phase to enter exponential growth, we assessed whether rigidification is reversible by observing if stationary-state BR-bodies fluidize

over time after nutrient replenishment (Extended Data Fig. 7). Indeed, BR-body disassembly was detected after 90 min of nutrient replenishment. We further investigated transcript storage by BR-bodies post-nutrient replenishment by monitoring the colocalization of the *spmX* transcript with BR-bodies in stationary phase cultures (Extended Data Fig. 8). After 3 hrs, the colocalization profile of *spmX* with BR-bodies returns to that observed during exponential phase (i.e., PCC = 0.22 ± 0.05 vs. 0.25 ± 0.04 in Fig. 3b), suggesting that stored mRNA exits BR-bodies upon removal of stress. Additionally, we evaluated if these transcripts could be translated after exiting BR-bodies. We replenished nutrients in stationary-phase cultures of *C. crescentus* cells with wild-type RNE and RNE-ΔCTD (incapable of forming BR-bodies),[11] inhibited new transcript synthesis with rifampicin, and monitored RNE-mEos3.2 and RNE-ΔCTD-mEos3.2 fluorescence (Fig. 4a). 6 hrs following bleaching of the whole cell intensity, RNE-ΔCTD cells recovered only minimally, while wild-type RNE cells recovered nearly completely (Fig. 4b). To ensure that the observed recovery was due to the translation of stored transcripts rather than protein maturation, we compared this result to the fluorescence recovery in cells having translation inhibited by chloramphenicol. This control resulted in minimal recovery, confirming that the recovery observed when transcript synthesis was inhibited is indeed due to the translation of *rne* transcripts released from BR-bodies following nutrient replenishment. Notably, the same behavior was observed for the *spmX* transcripts (Fig. 4a,b), indicating a general phenomenon. To confirm the presence of full-length mRNA that is capable of translation within the stationary phase BR-body, we amplified the full-length *ctrA* mRNA by RT-PCR and found that full-length mRNA is indeed present within the BR-body (Extended data Fig. 5c). The observed translation of released mRNA from BR-bodies suggests that BR-bodies can functionally store intact mRNAs for later translation upon stress removal.

We ultimately assessed the functional implications of mRNA storage in BR-bodies by comparing the growth rates of *C. crescentus* cells with wild-type RNE to those with RNE-ΔCTD after

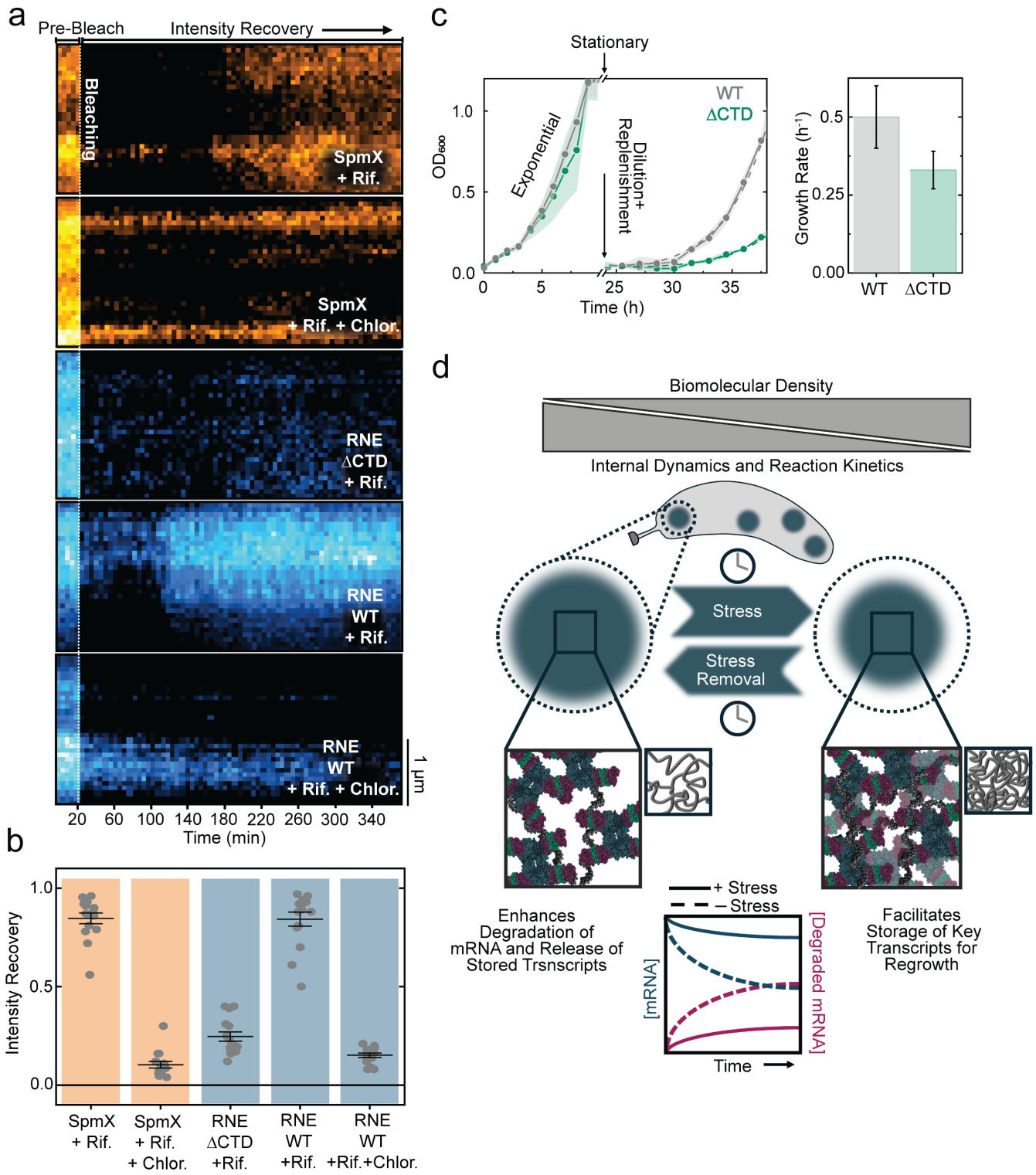


**Fig. 4 | Stored mRNAs can be translated and promote rapid growth.**

**Fig. 4 | Stored mRNAs can be translated and promote rapid growth.** (a) Representative kymographs of SpmX-mEos3.2, ΔCTD-RNE-mEos3.2, and wild-type RNE-mEos3.2 whole cell intensities in stationary phase cultures of *C. crescentus* cells after nutrient replenishment and inhibition of new transcript synthesis and translation with rifampicin and chloramphenicol, respectively. (b) Quantification of the recovery of the integrated intensity over the whole cell area at $t$ = 6 h relative to $t$ = 0 h following photobleaching of the whole cell intensity. Each dot below the distribution corresponds to the recovered intensity in one cell, and the error bars represent the standard error. (c) Functional implications of mRNA storage in BR-bodies. Left: comparison of the growth rate of *C. crescentus* cells with wild-type RNE vs. cells with RNE-ΔCTD (incapable of forming BR-bodies) when cultures are back-diluted into PYE medium after 24 h in the stationary phase. Right: growth rates following nutrient replenishment. Cells expressing RNE-ΔCTD grow more slowly following nutrient replenishment. (d) Proposed model showing how the material state of BR-bodies tunes their activity, enabling a transition from mRNA decay enhancement during growth to storage during stress.

24 hrs in the stationary phase (Fig. 4c). Remarkably, cells with RNE-ΔCTD exhibit a 1.5-fold reduction in growth rate and a lag phase that is 3 hrs longer compared to the wild-type strain following nutrient replenishment. These results suggest that during stress, BR-bodies play a critical role in storing essential transcripts, which are then readily available for translation upon return to nutrient-repleted conditions, in addition to promoting a faster transition into exponential growth. This storage mechanism circumvents the need to synthesize new transcripts, thereby facilitating the rapid program of protein production necessary for regrowth. Importantly, we observed in *Agrobacterium tumefaciens* and *Sinorhizobium meliloti* liquid-like BR-bodies also rigidify in the stationary phase (Extended Data Fig. 9), suggesting that the material state transition to mRNA storage may be a general feature of BR-bodies.

**Discussion**

BR-bodies are multifunctional biomolecular condensates that orchestrate RNA decay and store RNA transcripts during stress (Fig. 4d). Under prolonged stress, BR-bodies rigidify, resulting in decreased internal dynamics, higher biomolecular density, and compaction. This transition extends the residence time of RNE within these condensates, reduces its degradation activity, and leads to an altered degradosome. Consequently, RNA transcripts within BR-bodies are stabilized under adverse conditions.

The stabilization of mRNA within BR-bodies is a functional bacterial adaptation that allows the preservation of valuable epigenetic information during exposure to a variety of different stressors. Upon stress removal, environmental and cellular conditions shift, triggering the relaxation and disassembly of BR-bodies. This change facilitates the release of stabilized transcripts back into the cytoplasm, where they can be promptly translated to support recovery and growth. This elegant mechanism, wherein bacteria dynamically modulate the physical and biochemical properties of BR-

bodies in response to environmental cues, leverages phase separation and enzyme kinetics to exert temporal and spatial control over RNA degradation and utilization. This mechanism underscores how bacteria use biomolecular condensates not just as reaction sites but also as adaptive tools for managing genetic resources to ensure survival and adaptation in fluctuating environments.

The bacterial aggresome is another subcellular organelle that has recently been reported to store mRNA under arsenic stress in *E. coli*.[12,13,80] Our results indicate that, like aggresomes, BR-bodies store mRNA transcripts during stress conditions. However, the putative mechanisms by which aggresomes and BR-bodies stabilize mRNA differ significantly from one another. Aggresomes have been proposed to protect mRNA by excluding ribonucleases, with protein surface charge playing a crucial role.[80] Aggresomes are thought to occur through protein aggregation, and although protein chaperones are enriched within aggresome structures, the molecular trigger has not been uncovered.[12] However, whether aggresomes in *E. coli* might exclude RNE,[81–83] the major mRNA decay nuclease, has not yet been explored. In contrast, RNE is the central scaffold necessary for BR-body formation,[11] and rather than RNE being excluded from mature BR-bodies, the material properties of the BR-bodies shut off the RNase activity. Interestingly, *C. crescentus* BR-bodies have been found to enrich the aggresome marker proteins HslU, DnaK, and ClpB,[43] suggesting some functional similarity to aggresomes, yet aggresomes have a dark color in phase-contrast microscopy whereas no such dark aggregateshave been observed in *C. crescentus* at stationary phase nor following heat shock, antibiotic treatment, and other stresses.[11,35]

Despite the mechanistic data in the current study, it is still unclear how mRNA stored within BR-bodies is protected from RNE cleavage when cells transition from the stationary to the exponential phase. Potential models for future research include the possibility that *C. crescentus* possesses RNE inhibitor proteins stored within BR-bodies, similar to *E. coli* RraA and RraB.[84,85] Another hypothesis is that the RNE catalytic domain is completely denatured during rigidification

and requires refolding by protein or chaperones to become active again during the transition back to exponential growth.

Overall, we have determined that the function of the BR-bodies as sites of mRNA storage or decay is dictated by their material state. This model of BR-bodies underscores their role as versatile biomolecular condensates and also demonstrates how biophysical properties influence the biochemical function of condensates. The ability to modulate enzymatic activity through controlled biophysical changes within these condensates reveals a novel paradigm of gene expression regulation, which is pivotal for bacterial survival in fluctuating environments.

**Acknowledgments**

The authors acknowledge the support of NIH grant R35GM124733 to J.M.S., NIH T32GM142519-03 to HY., and NIH grants R01GM143182 and R01GM144731 to J.S.B. The authors thank Dr. Anthony Vecchiarelli for generously providing access to his wide-field fluorescence microscope. Thanks to Dr. Tamara Hendrickson and the WSU Department of Chemistry for lab space and equipment after the Schrader lab was destroyed in a fire.

The authors declare no competing interests.

**Author contributions**

L.A.O.-R. designed, performed and analyzed experiments (all live-cell single-molecule and ensemble fluorescence imaging, FRAP, FISH, growth curves and ATP level measurements), interpreted results and wrote the manuscript. H.Y. designed, performed and analyzed experiments (strain construction and BONCAT) and interpreted results. V.N. designed, performed and analyzed experiments (all *in vitro*-reconstitution experiments) and interpreted results. C.A.A. analyzed experiments (developed a script to isolate trajectories inside the condensates) and contributed to

writing the revised manuscript. J.C. analyzed experiments (cluster analysis). J.M.S. provided expertise in the design and construction of the strains, interpreted results and wrote the manuscript. J.S.B. provided expertise in the design of live-cell imaging experiments, designed experiments, interpreted results and wrote the manuscript.

**References**


1. Banani, S. F., Lee, H. O., Hyman, A. A. & Rosen, M. K. Biomolecular condensates: organizers of cellular biochemistry. *Nat. Rev. Mol. Cell Biol.* **18,** 285–298 (2017).
2. Boeynaems, S., Alberti, S., Fawzi, N. L., Mittag, T., Polymenidou, M., Rousseau, F., Schymkowitz, J., Shorter, J., Wolozin, B., Bosch, L. V. D., Tompa, P. & Fuxreiter, M. Protein Phase Separation: A New Phase in Cell Biology. *Trends Cell Biol.* **28,** 420–435 (2018).
3. Yoo, H., Triandafillou, C. & Drummond, D. A. Cellular sensing by phase separation: Using the process, not just the products. *J. Biol. Chem.* **294,** 7151–7159 (2019).
4. Ditlev, J. A., Case, L. B. & Rosen, M. K. Who's In and Who's Out—Compositional Control of Biomolecular Condensates. *J. Mol. Biol.* **430,** 4666–4684 (2018).
5. Nakamura, H., DeRose, R. & Inoue, T. Harnessing biomolecular condensates in living cells. *J. Biochem. (Tokyo)* **166,** 13–27 (2019).
6. Aguzzi, A. & Altmeyer, M. Phase Separation: Linking Cellular Compartmentalization to Disease. *Trends Cell Biol.* **26,** 547–558 (2016).
7. Ramaswami, M., Taylor, J. P. & Parker, R. Altered Ribostasis: RNA-Protein Granules in Degenerative Disorders. *Cell* **154,** 727–736 (2013).

8. Zhu, L., Richardson, T. M., Wacheul, L., Wei, M.-T., Feric, M., Whitney, G., Lafontaine, D. L. J. & Brangwynne, C. P. Controlling the material properties and rRNA processing function of the nucleolus using light. *Proc. Natl. Acad. Sci.* **116,** 17330–17335 (2019).
9. Dorone, Y., Boeynaems, S., Flores, E., Jin, B., Hateley, S., Bossi, F., Lazarus, E., Pennington, J. G., Michiels, E., Decker, M. D., Vints, K., Baatsen, P., Bassel, G. W., Otegui, M. S., Holehouse, A. S., Exposito-Alonso, M., Sukenik, S., Gitler, A. D. & Rhee, S. Y. A prion-like protein regulator of seed germination undergoes hydration-dependent phase separation. *Cell* **184,** 4284-4298.e27 (2021).
10. Bose, M., Lampe, M., Mahamid, J. & Ephrussi, A. Liquid-to-solid phase transition of *oskar* ribonucleoprotein granules is essential for their function in *Drosophila* embryonic development. *Cell* **185,** 1308-1324.e23 (2022).
11. Al-Husini, N., Tomares, D. T., Bitar, O., Childers, W. S. & Schrader, J. M. α-Proteobacterial RNA Degradosomes Assemble Liquid-Liquid Phase-Separated RNP Bodies. *Mol. Cell* **71,** 1027-1039.e14 (2018).
12. Pu, Y., Li, Y., Jin, X., Tian, T., Ma, Q., Zhao, Z., Lin, S., Chen, Z., Li, B., Yao, G., Leake, M. C., Lo, C.-J. & Bai, F. ATP-Dependent Dynamic Protein Aggregation Regulates Bacterial Dormancy Depth Critical for Antibiotic Tolerance. *Mol. Cell* **73,** 143-156.e4 (2019).
13. Jin, X., Lee, J.-E., Schaefer, C., Luo, X., Wollman, A. J. M., Payne-Dwyer, A. L., Tian, T., Zhang, X., Chen, X., Li, Y., McLeish, T. C. B., Leake, M. C. & Bai, F. Membraneless organelles formed by liquid-liquid phase separation increase bacterial fitness. *Sci. Adv.* **7,** eabh2929 (2021).

14. Heinkel, F., Abraham, L., Ko, M., Chao, J., Bach, H., Hui, L. T., Li, H., Zhu, M., Ling, Y. M., Rogalski, J. C., Scurll, J., Bui, J. M., Mayor, T., Gold, M. R., Chou, K. C., Av-Gay, Y., McIntosh, L. P. & Gsponer, J. Phase separation and clustering of an ABC transporter in Mycobacterium tuberculosis. *Proc. Natl. Acad. Sci.* **116,** 16326–16331 (2019).
15. MacCready, J. S., Basalla, J. L. & Vecchiarelli, A. G. Origin and Evolution of Carboxysome Positioning Systems in Cyanobacteria. *Mol. Biol. Evol.* **37,** 1434–1451 (2020).
16. McQuail, J., Carpousis, A. J. & Wigneshweraraj, S. The association between Hfq and RNase E in long-term nitrogen-starved Escherichia coli. *Mol. Microbiol.* **117,** 54–66 (2022).
17. Azaldegui, C. A., Vecchiarelli, A. G. & Biteen, J. S. The emergence of phase separation as an organizing principle in bacteria. *Biophys. J.* **120,** 1123–1138 (2021).
18. Saurabh, S., Chong, T. N., Bayas, C., Dahlberg, P. D., Cartwright, H. N., Moerner, W. E. & Shapiro, L. ATP-responsive biomolecular condensates tune bacterial kinase signaling. *Sci. Adv.* **8,** eabm6570 (2022).
19. Lasker, K., von Diezmann, L., Zhou, X., Ahrens, D. G., Mann, T. H., Moerner, W. E. & Shapiro, L. Selective sequestration of signalling proteins in a membraneless organelle reinforces the spatial regulation of asymmetry in Caulobacter crescentus. *Nat. Microbiol.* **5,** 418–429 (2020).
20. Surovtsev, I. V. & Jacobs-Wagner, C. Subcellular Organization: A Critical Feature of Bacterial Cell Replication. *Cell* **172,** 1271–1293 (2018).

21. Treuner-Lange, A. & Søgaard-Andersen, L. Regulation of cell polarity in bacteria. *J. Cell Biol.* **206,** 7–17 (2014).

22. Hammarlöf, D. L., Bergman, J. M., Garmendia, E. & Hughes, D. Turnover of mRNAs is one of the essential functions of RNase E. *Mol. Microbiol.* **98,** 34–45 (2015).

23. Ono, M. & Kuwano, M. A conditional lethal mutation in an *Escherichia coli* strain with a longer chemical lifetime of messenger RNA. *J. Mol. Biol.* **129,** 343–357 (1979).

24. Kedersha, N., Stoecklin, G., Ayodele, M., Yacono, P., Lykke-Andersen, J., Fritzler, M. J., Scheuner, D., Kaufman, R. J., Golan, D. E. & Anderson, P. Stress granules and processing bodies are dynamically linked sites of mRNP remodeling. *J. Cell Biol.* **169,** 871–884 (2005).

25. Hubstenberger, A., Courel, M., Bénard, M., Souquere, S., Ernoult-Lange, M., Chouaib, R., Yi, Z., Morlot, J.-B., Munier, A., Fradet, M., Daunesse, M., Bertrand, E., Pierron, G., Mozziconacci, J., Kress, M. & Weil, D. P-Body Purification Reveals the Condensation of Repressed mRNA Regulons. *Mol. Cell* **68,** 144-157.e5 (2017).

26. Youn, J.-Y., Dyakov, B. J. A., Zhang, J., Knight, J. D. R., Vernon, R. M., Forman-Kay, J. D. & Gingras, A.-C. Properties of Stress Granule and P-Body Proteomes. *Mol. Cell* **76,** 286–294 (2019).

27. Rathnayaka-Mudiyanselage, I., Nandana, V. & Schrader, J. Proteomic composition of eukaryotic and bacterial RNA decay condensates suggests convergent evolution. *Curr. Opin. Microbiol.* **79,** 102467 (2024).

28. Brengues, M., Teixeira, D. & Parker, R. Movement of Eukaryotic mRNAs Between Polysomes and Cytoplasmic Processing Bodies. *Science* **310,** 486–489 (2005).

29. Sheth, U. & Parker, R. Decapping and Decay of Messenger RNA Occur in Cytoplasmic Processing Bodies. *Science* **300,** 805–808 (2003).

30. Xing, W., Muhlrad, D., Parker, R. & Rosen, M. K. A quantitative inventory of yeast P body proteins reveals principles of composition and specificity. *eLife* **9,** e56525 (2020).

31. Blake, L. A., Watkins, L., Liu, Y., Inoue, T. & Wu, B. A rapid inducible RNA decay system reveals fast mRNA decay in P-bodies. *Nat. Commun.* **15,** 2720 (2024).

32. Wheeler, J. R., Matheny, T., Jain, S., Abrisch, R. & Parker, R. Distinct stages in stress granule assembly and disassembly. *eLife* **5,** e18413 (2016).

33. Moon, S. L., Morisaki, T., Khong, A., Lyon, K., Parker, R. & Stasevich, T. J. Multicolour single-molecule tracking of mRNA interactions with RNP granules. *Nat. Cell Biol.* **21,** 162–168 (2019).

34. Mateju, D., Franzmann, T. M., Patel, A., Kopach, A., Boczek, E. E., Maharana, S., Lee, H. O., Carra, S., Hyman, A. A. & Alberti, S. An aberrant phase transition of stress granules triggered by misfolded protein and prevented by chaperone function. *EMBO J.* **36,** 1669–1687 (2017).

35. Al-Husini, N., Tomares, D. T., Pfaffenberger, Z. J., Muthunayake, N. S., Samad, M. A., Zuo, T., Bitar, O., Aretakis, J. R., Bharmal, M.-H. M., Gega, A., Biteen, J. S., Childers, W. S. & Schrader, J. M. BR-Bodies Provide Selectively Permeable Condensates that Stimulate mRNA Decay and Prevent Release of Decay Intermediates. *Mol. Cell* **78,** 670-682.e8 (2020).

36. Chen, H., Shiroguchi, K., Ge, H. & Xie, X. S. Genome-wide study of mRNA degradation and transcript elongation in Escherichia coli. *Mol. Syst. Biol.* **11,** 781 (2015).

37. Barnett, T. C., Bugrysheva, J. V. & Scott, J. R. Role of mRNA Stability in Growth Phase Regulation of Gene Expression in the Group A Streptococcus. *J. Bacteriol.* **189,** 1866–1873 (2007).

38. Hambraeus, G., von Wachenfeldt, C. & Hederstedt, L. Genome-wide survey of mRNA half-lives in Bacillus subtilis identifies extremely stable mRNAs. *Mol. Genet. Genomics* **269,** 706–714 (2003).

39. Dressaire, C., Pobre, V., Laguerre, S., Girbal, L., Arraiano, C. M. & Cocaign-Bousquet, M. PNPase is involved in the coordination of mRNA degradation and expression in stationary phase cells of Escherichia coli. *BMC Genomics* **19,** 848 (2018).

40. Esquerré, T., Laguerre, S., Turlan, C., Carpousis, A. J., Girbal, L. & Cocaign-Bousquet, M. Dual role of transcription and transcript stability in the regulation of gene expression in Escherichia coli cells cultured on glucose at different growth rates. *Nucleic Acids Res.* **42,** 2460–2472 (2014).

41. Morrison, J. M., Anderson, K. L., Beenken, K. E., Smeltzer, M. S. & Dunman, P. M. The staphylococcal accessory regulator, SarA, is an RNA-binding protein that modulates the mRNA turnover properties of late-exponential and stationary phase Staphylococcus aureus cells. *Front. Cell. Infect. Microbiol.* **2,** (2012).

42. Zhang, M., Chang, H., Zhang, Y., Yu, J., Wu, L., Ji, W., Chen, J., Liu, B., Lu, J., Liu, Y., Zhang, J., Xu, P. & Xu, T. Rational design of true monomeric and bright photoactivatable fluorescent proteins. *Nat. Methods* **9,** 727–729 (2012).

43. Nandana, V., Rathnayaka-Mudiyanselage, I. W., Muthunayake, N. S., Hatami, A., Mousseau, C. B., Ortiz-Rodríguez, L. A., Vaishnav, J., Collins, M., Gega, A.,

Mallikaarachchi, K. S., Yassine, H., Ghosh, A., Biteen, J. S., Zhu, Y., Champion, M. M., Childers, W. S. & Schrader, J. M. The BR-body proteome contains a complex network of protein-protein and protein-RNA interactions. *Cell Rep.* **42,** (2023).

44. Hardwick, S. W., Chan, V. S. Y., Broadhurst, R. W. & Luisi, B. F. An RNA degradosome assembly in Caulobacter crescentus. *Nucleic Acids Res.* **39,** 1449–1459 (2011).
45. Ester, M., Kriegel, H.-P., Sander, J. & Xu, X. A density-based algorithm for discovering clusters in large spatial databases with noise. in *Proc. Second Int. Conf. Knowl. Discov. Data Min.* 226–231 (AAAI Press, 1996).
46. Hondele, M., Sachdev, R., Heinrich, S., Wang, J., Vallotton, P., Fontoura, B. M. A. & Weis, K. DEAD-box ATPases are global regulators of phase-separated organelles. *Nature* **573,** 144–148 (2019).
47. Deng, Y., Beahm, D. R., Ionov, S. & Sarpeshkar, R. Measuring and modeling energy and power consumption in living microbial cells with a synthetic ATP reporter. *BMC Biol.* **19,** 101 (2021).
48. Parry, B. R., Surovtsev, I. V., Cabeen, M. T., O'Hern, C. S., Dufresne, E. R. & Jacobs-Wagner, C. The Bacterial Cytoplasm Has Glass-like Properties and Is Fluidized by Metabolic Activity. *Cell* **156,** 183–194 (2014).
49. Weber, S. C., Spakowitz, A. J. & Theriot, J. A. Nonthermal ATP-dependent fluctuations contribute to the in vivo motion of chromosomal loci. *Proc. Natl. Acad. Sci.* **109,** 7338–7343 (2012).
50. Li, X.-Z., Plésiat, P. & Nikaido, H. The Challenge of Efflux-Mediated Antibiotic Resistance in Gram-Negative Bacteria. *Clin. Microbiol. Rev.* **28,** 337–418 (2015).

51. Nathans, D. Puromycin inhibition of protein synthesis: incorporation of puromycin into peptide chains. *Proc. Natl. Acad. Sci.* **51,** 585–592 (1964).

52. Oh, E., Becker, A. H., Sandikci, A., Huber, D., Chaba, R., Gloge, F., Nichols, R. J., Typas, A., Gross, C. A., Kramer, G., Weissman, J. S. & Bukau, B. Selective Ribosome Profiling Reveals the Cotranslational Chaperone Action of Trigger Factor In Vivo. *Cell* **147,** 1295–1308 (2011).

53. Pontes, M. H., Sevostyanova, A. & Groisman, E. A. When Too Much ATP Is Bad for Protein Synthesis. *J. Mol. Biol.* **427,** 2586–2594 (2015).

54. Stouthamer, A. H. A theoretical study on the amount of ATP required for synthesis of microbial cell material. *Antonie Van Leeuwenhoek* **39,** 545–565 (1973).

55. Patel, A., Lee, H. O., Jawerth, L., Maharana, S., Jahnel, M., Hein, M. Y., Stoynov, S., Mahamid, J., Saha, S., Franzmann, T. M., Pozniakovski, A., Poser, I., Maghelli, N., Royer, L. A., Weigert, M., Myers, E. W., Grill, S., Drechsel, D., Hyman, A. A. & Alberti, S. A Liquid-to-Solid Phase Transition of the ALS Protein FUS Accelerated by Disease Mutation. *Cell* **162,** 1066–1077 (2015).

56. Molliex, A., Temirov, J., Lee, J., Coughlin, M., Kanagaraj, A. P., Kim, H. J., Mittag, T. & Taylor, J. P. Phase Separation by Low Complexity Domains Promotes Stress Granule Assembly and Drives Pathological Fibrillization. *Cell* **163,** 123–133 (2015).

57. Zhang, H., Elbaum-Garfinkle, S., Langdon, E. M., Taylor, N., Occhipinti, P., Bridges, A. A., Brangwynne, C. P. & Gladfelter, A. S. RNA Controls PolyQ Protein Phase Transitions. *Mol. Cell* **60,** 220–230 (2015).

58. Lin, Y., Protter, D. S. W., Rosen, M. K. & Parker, R. Formation and Maturation of Phase-Separated Liquid Droplets by RNA-Binding Proteins. *Mol. Cell* **60,** 208–219 (2015).

59. Xiang, S., Kato, M., Wu, L. C., Lin, Y., Ding, M., Zhang, Y., Yu, Y. & McKnight, S. L. The LC Domain of hnRNPA2 Adopts Similar Conformations in Hydrogel Polymers, Liquid-like Droplets, and Nuclei. *Cell* **163,** 829–839 (2015).

60. Watanabe, H. Viscoelasticity and dynamics of entangled polymers. *Prog. Polym. Sci.* **24,** 1253–1403 (1999).

61. Halfmann, R. A glass menagerie of low complexity sequences. *Curr. Opin. Struct. Biol.* **38,** 18–25 (2016).

62. Mittag, T. & Pappu, R. V. A conceptual framework for understanding phase separation and addressing open questions and challenges. *Mol. Cell* **82,** 2201–2214 (2022).

63. Boke, E., Ruer, M., Wühr, M., Coughlin, M., Lemaitre, R., Gygi, S. P., Alberti, S., Drechsel, D., Hyman, A. A. & Mitchison, T. J. Amyloid-like Self-Assembly of a Cellular Compartment. *Cell* **166,** 637–650 (2016).

64. Linsenmeier, M., Hondele, M., Grigolato, F., Secchi, E., Weis, K. & Arosio, P. Dynamic arrest and aging of biomolecular condensates are modulated by low-complexity domains, RNA and biochemical activity. *Nat. Commun.* **13,** 3030 (2022).

65. Bertrand, E., Chartrand, P., Schaefer, M., Shenoy, S. M., Singer, R. H. & Long, R. M. Localization of ASH1 mRNA Particles in Living Yeast. *Mol. Cell* **2,** 437–445 (1998).

66. Tutucci, E., Vera, M., Biswas, J., Garcia, J., Parker, R. & Singer, R. H. An improved MS2 system for accurate reporting of the mRNA life cycle. *Nat. Methods* **15,** 81–89 (2018).

67. Awram, P. & Smit, J. The Caulobacter crescentus Paracrystalline S-Layer Protein Is Secreted by an ABC Transporter (Type I) Secretion Apparatus. *J. Bacteriol.* **180,** 3062–3069 (1998).

68. Wheeler, R. T. & Shapiro, L. Differential Localization of Two Histidine Kinases Controlling Bacterial Cell Differentiation. *Mol. Cell* **4,** 683–694 (1999).

69. Radhakrishnan, S. K., Thanbichler, M. & Viollier, P. H. The dynamic interplay between a cell fate determinant and a lysozyme homolog drives the asymmetric division cycle of Caulobacter crescentus. *Genes Dev.* **22,** 212–225

70. Ryan, K. R., Judd, E. M. & Shapiro, L. The CtrA Response Regulator Essential for *Caulobacter crescentus* Cell-cycle Progression Requires a Bipartite Degradation Signal for Temporally Controlled Proteolysis. *J. Mol. Biol.* **324,** 443–455 (2002).

71. Wortinger, M., Sackett, M. J. & Brun, Y. V. CtrA mediates a DNA replication checkpoint that prevents cell division in Caulobacter crescentus. *EMBO J.* **19,** 4503–4512 (2000).

72. Laub, M. T., Chen, S. L., Shapiro, L. & McAdams, H. H. Genes directly controlled by CtrA, a master regulator of the Caulobacter cell cycle. *Proc. Natl. Acad. Sci.* **99,** 4632–4637 (2002).

73. Laub, M. T., McAdams, H. H., Feldblyum, T., Fraser, C. M. & Shapiro, L. Global Analysis of the Genetic Network Controlling a Bacterial Cell Cycle. *Science* **290,** 2144–2148 (2000).

74. Quon, K. C., Marczynski, G. T. & Shapiro, L. Cell Cycle Control by an Essential Bacterial Two-Component Signal Transduction Protein. *Cell* **84,** 83–93 (1996).

75. LeCuyer, K. A., Behlen, L. S. & Uhlenbeck, O. C. Mutants of the Bacteriophage MS2 Coat Protein That Alter Its Cooperative Binding to RNA. *Biochemistry* **34,** 10600–10606 (1995).

76. Garcia, J. F. & Parker, R. MS2 coat proteins bound to yeast mRNAs block 5' to 3' degradation and trap mRNA decay products: implications for the localization of mRNAs by MS2-MCP system. *RNA* **21,** 1393–1395 (2015).

77. Heinrich, S., Sidler, C. L., Azzalin, C. M. & Weis, K. Stem–loop RNA labeling can affect nuclear and cytoplasmic mRNA processing. *RNA* **23,** 134–141 (2017).

78. Garcia, J. F. & Parker, R. Ubiquitous accumulation of 3' mRNA decay fragments in Saccharomyces cerevisiae mRNAs with chromosomally integrated MS2 arrays. *RNA* **22,** 657 (2016).

79. Nandana, V., Al-Husini, N., Vaishnav, A., Dilrangi, K. H. & Schrader, J. M. Caulobacter crescentus RNase E condensation contributes to autoregulation and fitness. *Mol. Biol. Cell* **35,** ar104 (2024).

80. Pei, L., Xian, Y., Yan, X., Schaefer, C., Syeda, A. H., Howard, J., Liao, H., Bai, F., Leake, M. C. & Pu, Y. Bacterial stress granule protects mRNA through ribonucleases exclusion. 2024.04.27.591437 Preprint at https://doi.org/10.1101/2024.04.27.591437 (2024)

81. Mudd, E. A., Krisch, H. M. & Higgins, C. F. RNase E, an endoribonuclease, has a general role in the chemical decay of Escherichia coli mRNA: evidence that rne and ams are the same genetic locus. *Mol. Microbiol.* **4,** 2127–2135 (1990).

82. Górna, M. W., Carpousis, A. J. & Luisi, B. F. From conformational chaos to robust regulation: the structure and function of the multi-enzyme RNA degradosome. *Q. Rev. Biophys.* **45,** 105–145 (2012).

83. Bandyra, K. J., Bouvier, M., Carpousis, A. J. & Luisi, B. F. The social fabric of the RNA degradosome. *Biochim. Biophys. Acta BBA - Gene Regul. Mech.* **1829,** 514–522 (2013).

84. Lee, K., Zhan, X., Gao, J., Qiu, J., Feng, Y., Meganathan, R., Cohen, S. N. & Georgiou, G. RraA: a Protein Inhibitor of RNase E Activity that Globally Modulates RNA Abundance in E. coli. *Cell* **114,** 623–634 (2003).

85. Górna, M. W., Pietras, Z., Tsai, Y.-C., Callaghan, A. J., Hernández, H., Robinson, C. V. & Luisi, B. F. The regulatory protein RraA modulates RNA-binding and helicase activities of the E. coli RNA degradosome. *RNA* **16,** 553–562 (2010).

86. Thanbichler, M., Iniesta, A. A. & Shapiro, L. A comprehensive set of plasmids for vanillate- and xylose-inducible gene expression in Caulobacter crescentus. *Nucleic Acids Res.* **35,** e137 (2007).

87. Schrader, J. M. & Shapiro, L. Synchronization of Caulobacter Crescentus for Investigation of the Bacterial Cell Cycle. *J. Vis. Exp. JoVE* e52633 (2015). doi:10.3791/52633

88. Ducret, A., Quardokus, E. M. & Brun, Y. V. MicrobeJ, a tool for high throughput bacterial cell detection and quantitative analysis. *Nat. Microbiol.* **1,** 1–7 (2016).

89. Schindelin, J., Arganda-Carreras, I., Frise, E., Kaynig, V., Longair, M., Pietzsch, T., Preibisch, S., Rueden, C., Saalfeld, S., Schmid, B., Tinevez, J.-Y., White, D. J.,

Hartenstein, V., Eliceiri, K., Tomancak, P. & Cardona, A. Fiji: an open-source platform for biological-image analysis. *Nat. Methods* **9,** 676–682 (2012).

90. Isaacoff, B. P., Li, Y., Lee, S. A. & Biteen, J. S. SMALL-LABS: Measuring Single-Molecule Intensity and Position in Obscuring Backgrounds. *Biophys. J.* **116,** 975–982 (2019).
91. Endesfelder, U., Malkusch, S., Fricke, F. & Heilemann, M. A simple method to estimate the average localization precision of a single-molecule localization microscopy experiment. *Histochem. Cell Biol.* **141,** 629–638 (2014).
92. Miura, K. Bleach correction ImageJ plugin for compensating the photobleaching of time-lapse sequences. Preprint at https://doi.org/10.12688/f1000research.27171.1 (2020)